Available online at www.sciencedirect.com

jmr&t Journal of Materials Research and Technology

journal homepage: www.elsevier.com/locate/jmrt

Original Article

Structural, electronic and optical properties of the anhydrous orthorhombic $2C_{14}H_{12}Br_2S_3Bis$ (2-Bromobenzyl) trisulfide crystals

Z. Zerrougui [a], M.A. Ghebouli [b,c], T. Chihi [b], Sameh I. Ahmed [d], L. Krache [e], B. Ghebouli [a], M. Reffas [b], M. Fatmi [b,*]

[a] Laboratory of Surfaces and Interfaces Studies of Solid Materials, Faculty of Technology, University Ferhat Abbas of Setif 1, Setif, 19000, Algeria
[b] Research Unit on Emerging Materials (RUEM), University of Ferhat Abbas Setif 1, 19000 Algeria
[c] Department of Chemistry, Faculty of Technology, University of Mohamed Boudiaf, M'sila, 28000, Algeria
[d] Department of Physics, College of Science, Taif University, P.O. Box 11099, Taif 21944, Saudi Arabia
[e] PQSD Laboratory, Department of Physics, Faculty of Science, University of Ferhat Abbas Setif 1, 19000, Algeria

ARTICLE INFO

Article history:
Received 27 January 2022
Accepted 14 February 2022
Available online 22 February 2022

Keywords:
$C_{14}H_{12}Br_2S_3$ crystal
Optical absorption
Bromobenzyl
Trisulfide crystals
Band structure

ABSTRACT

The $C_{14}H_{12}Br_2S_3$ molecule has twofold imposed crystallographic symmetry in the solid state. $2C_{14}H_{12}Br_2S_3Bis$ (2-Bromobenzyl) trisulfide in the orthorhombic structure with space group $P2_12_12$ is described and compared with other similar compounds. The structural, electronic, and optical properties of the anhydrous orthorhombic $2C_{14}H_{12}Br_2S_3Bis$ (2-Bromobenzyl) trisulfide crystals were treated within LDA/CA-PZ, GGA/PBE and GGA/PW91 approaches. The lattice parameters calculated with LDA/CA-PZ ($a = 12.651$ Å, $b = 12.881$ Å and $c = 4.992$ Å) are in better agreement with experimental values, where the error is 0.90%, 1.14%, and 4.79% for a cutoff energy 240 eV. This calculation shows the usual trends, where the GGA/PBE and GGA/PW91 functional overestimate the lattice constant, unlike the LDA/CA-PZ. The $C_{14}H_{12}Br_2S_3$ molecule has a large indirect band gap $Z \rightarrow \Gamma$ of 3.4498 eV and 3.5319 eV computed within LDA/CA-PZ and GGA/PBE approaches. The hybridization in the upper valence band between S: p, B: p and C: p, translates their covalent bonding. The Mulliken population charges show the zwitterionic state of the $C_{14}H_{12}Br_2S_3$ molecule.

1. Introduction

The $C_{14}H_{12}Br_2S_3$ molecule is based on twofold crystallographic rotation axis, which bisects the S-S-S angles in the solid state. The dihedral angle between the two benzene ring symmetries is 89.91° [1,2]. This class of sulfur abundant in nature is very important in living chemistry. Organic sulfides are attracted researchers because of their synthetic and pharmaceutical applications. The structural stabilization of

* Corresponding author.
E-mail address: fatmimessaoud@yahoo.fr (M. Fatmi).
https://doi.org/10.1016/j.jmrt.2022.02.065

Table 1 – The atomic coordinates of $C_{14}H_{12}Br_2S_3$ calculated with LDA/CA-PZ are compared with available experimental ones.

Element	x (Å)	Exp (Å)	y (Å)	Exp (Å)	z (Å)	Exp (Å)
Br	0.4230	0.4224	0.3829	0.3803	0.1262	0.1301
S1	0.5000	0.5000	0.0000	0.0000	0.2404	0.2536
S2	0.5358	0.5373	0.1218	0.1197	−0.0028	−0.0036
C1	0.3280	0.3293	0.1824	0.1822	0.0646	0.0620
C2	0.3231	0.3222	0.2773	0.2750	0.2015	0.2054
C3	0.2476	0.2470	0.2967	0.2930	0.3963	0.4058
C4	0.1739	0.1750	0.2205	0.2117	0.4583	0.4693
C5	0.1782	0.1784	0.1245	0.1239	0.3335	0.3296
C6	0.2547	0.2529	0.1062	0.1057	0.1399	0.1324
C7	0.4089	0.4113	0.1599	0.1583	−0.1432	−0.1526
H1	0.2464	0.2446	0.3711	0.3572	0.5017	0.5002
H2	0.1137	0.1232	0.2355	0.2294	0.6115	0.6086
H3	0.1213	0.1282	0.0640	0.0724	0.3881	0.3722
H4	0.2567	0.2544	0.0313	0.0412	0.0357	0.0395
H5	0.3829	0.3853	0.0984	0.1024	−0.2827	−0.2750
H6	0.4295	0.4221	0.2301	0.2196	−0.2610	−0.2718

trisulfides makes them a perfect example in molecular recognition with self-complementary donor and acceptor units in a single molecule. This structure crystallizes in the orthorhombic structure, with space group $P2_12_12$. This type of molecule exhibits intramolecular and intermolecular H-bonding interactions. The experimental crystal data of $C_{14}H_{12}Br_2S_3$ molecule are $a = 12.771$ Å, $b = 13.030$ Å and $c = 4.7635$ Å [1,3], while he density and the atomic number are 1.7808 g cm^{-3} and z = 2. Our calculation using the LDA/CA-PZ approximation gives the lattice parameters $a = 12.651$ Å, $b = 12.881$ Å and $c = 4.992$ Å, which are practically closer to the experimental values. Also the computed S-S bond length of 2.036 Å is in good concordance with the experimental value of 2.04 Å. The selected bond angles S2-S1-S2 and C2-C1-S2 reported in the literature are 106.21° [4] and 114° [3]. The analysis of $C_{14}H_{12}Br_2S_3$ single crystal by X-ray diffraction conducted by Krishna P. Bhabak and Debasish Bhowmick reveals the stabilization of trisulfides and facilitates effective intramolecular as well as intermolecular non-covalent interactions [2]. S. P. Singh et al. synthesized and obtained single crystals of $2C_{14}H_{12}Br_2S_3$ [1], and then gave a detailed analysis of X-ray diffraction [5]. Organic sulfide is a group that is part of organosulfuric chemistry and is often associated with elements with a bad smell [6,7]. The derivatives and some biological activities have been synthesized and reported on anhydrous trisulfide crystals [8]. We focus in this work on the investigation of the structural, electronic and optical properties of the anhydrous orthorhombic $2C_{14}H_{12}Br_2S_3$Bis (2-Bromobenzyl) trisulfide crystals. We have used in this calculation a pseudo potential approach within the density functional theory (DFT). As exchange functional, we have considered both the generalized gradient approximation with dispersion correction GGA/PBE and GGA/PW91 and the local density approximation LDA/CA-PZ.

The organization of this paper is as follows: We explain the computational method in section 2. The results are presented and discussed in section 3. We conclude this work in section 4.

2. Computational details

The CASTEP code (version 7.0) [9] was used to achieve the DFT calculations of the orthorhombic $C_{14}H_{12}Br_2S_3$ unit cell. The exchange-correlation was presented by Ceperley-Alder-Perdew-Zunger (CAPZ) and Perdew-Burke-Ernzerhof (PBE) of generalized gradient approximation (GGA) [10–12]. The LDA is an approach derived from the homogeneous electronic gas model [13]. The valence electronic configuration of S, Br, C and

Table 2 – The lattice parameters, *c/a*, *c/b* ratios, volume, density, atomic number and energy of $C_{14}H_{12}Br_2S_3$ and their available experimental data.

$C_{14}H_{12}Br_2S_3$	Experiment [1]	LDA/CA-PZ (240; 5 × 5 × 5)	GGA/PBE (600; 8 × 8 × 8)	GGA/PW91 (600; 8 × 8 × 8)
Space group	$P2_12_12$ (N°18)	$P2_12_12$ (N°18)	$P2_12_12$ (N°18)	$P2_12_12$ (N°18)
***a* (Å)**	12.771	12.651 0.9	12.5965 1.3	12.6238 1.1
***b* (Å)**	13.030	12.881 1.1	13.4404 3	13.4679 3.2
c (Å)	4.7635	4.9918 4.5	5.0467 5.6	5.0669 5.9
c/a	0.3930	0.3945	0.4006	0.4014
c/b	0.3656	0.3875	0.3755	0.3762
Volume ($Å^3$)	792.7	813.52	854.44	861.48
Z	2	2	2	2
density ($g.cm^{-3}$)	1.828	1.78087	1.69560	1.68173
Atoms number	62	62	62	62
Energy eV	–	−7856.998	−7853.698	−7867.948

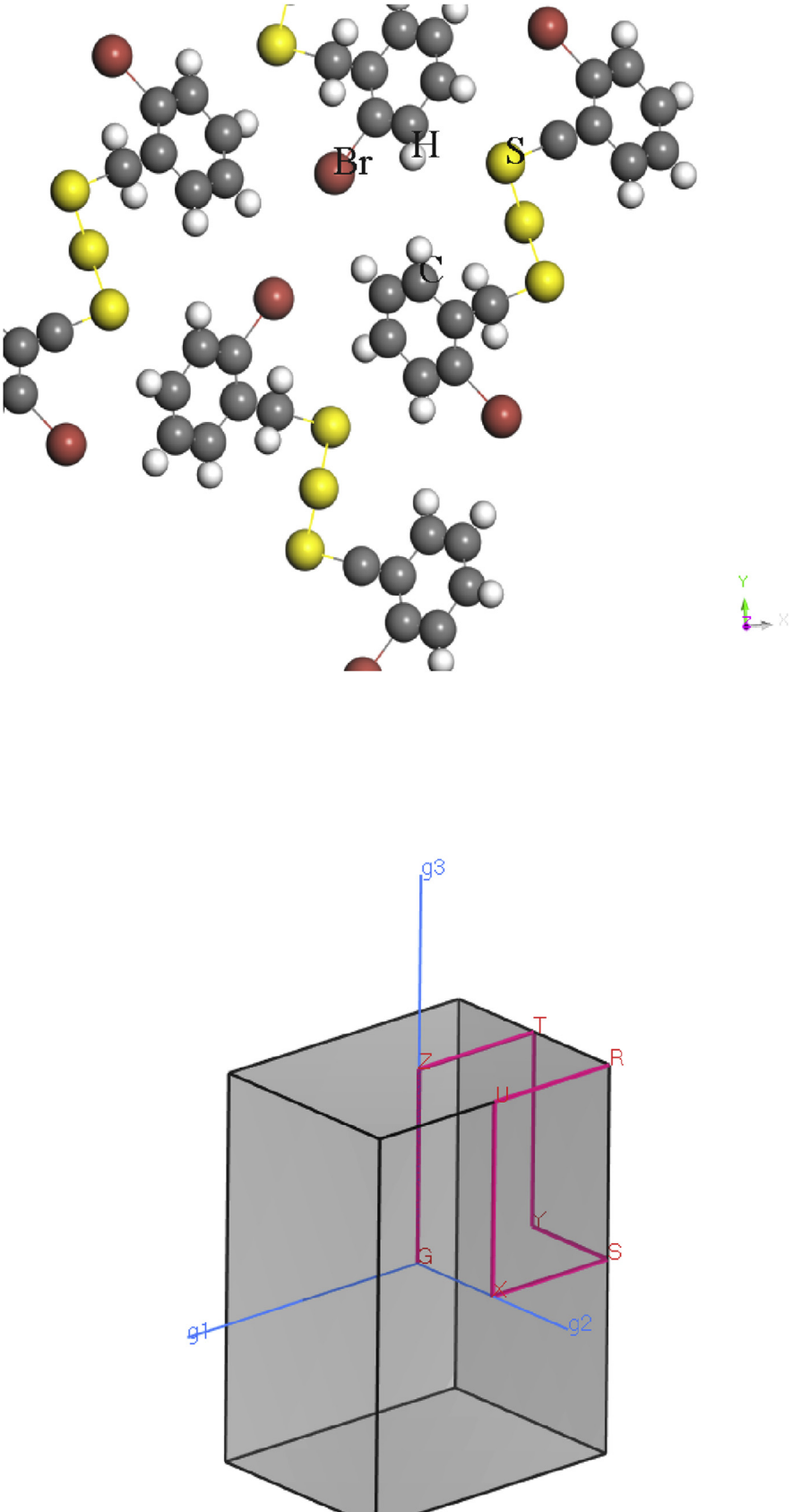

Fig. 1 – Orthorhombic crystal structure in the unit cell and Brillouin Zone of $C_{14}H_{12}Br_2S_3$ molecule.

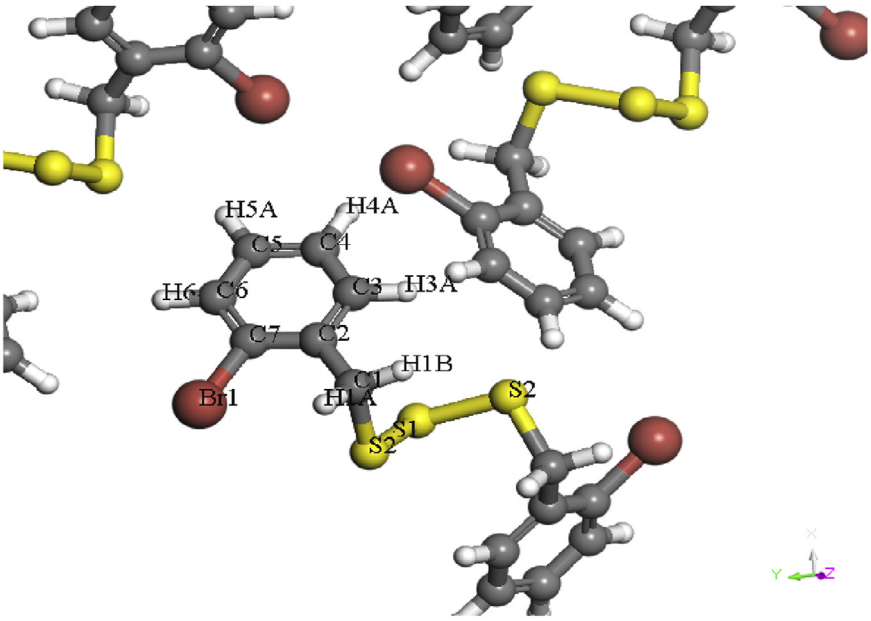

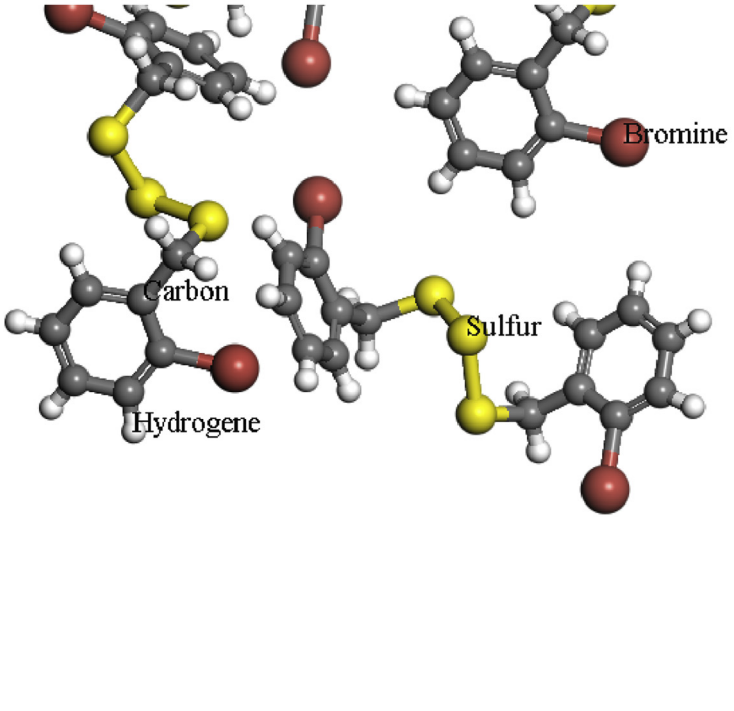

Fig. 2 – The $C_{14}H_{12}Br_2S_3$ molecule in the zwitterionic form.

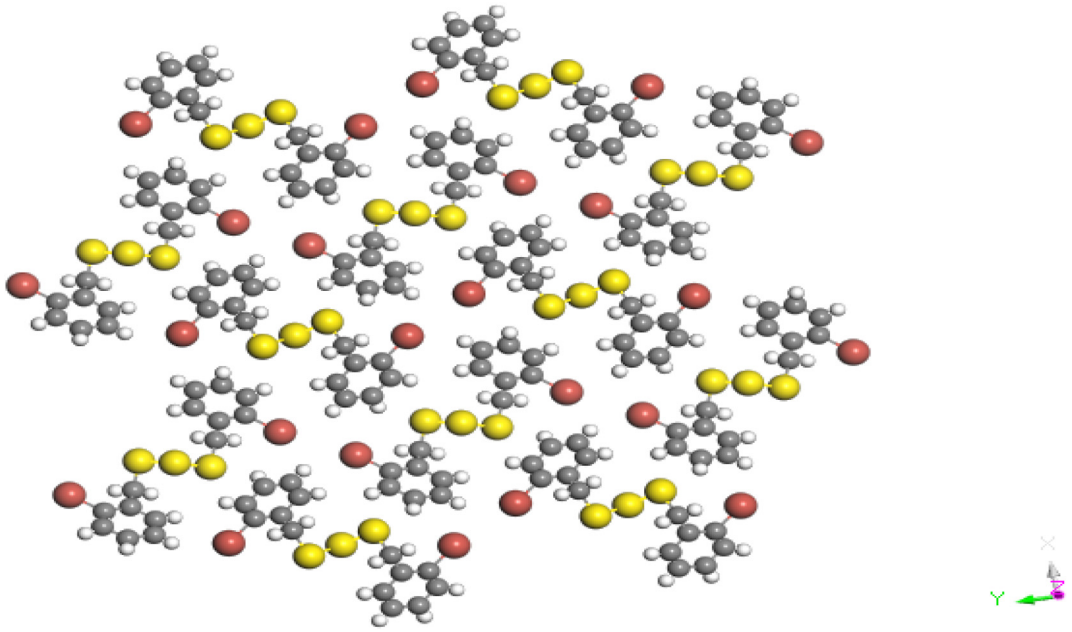

Fig. 3 – A perspective view of $C_{14}H_{12}Br_2S_3$ crystal structure.

H are $3p^4$, $4p^5$, $2p^2$ and $1s^1$. The cut-off energy is chosen 240 eV and the Monkhorst-Pack grid is set to 1 × 1 × 1 for the Brillouin zone to accomplish integration into the reciprocal space [14]. The $C_{14}H_{12}Br_2S_3$ structure has been optimized by seeking a minimum of total energy via a calculation with GGA/PBE, GGA/PW91 and LDA/CA-PZ [15–17]. The optimization geometry is such that one minimizes the stress and one finds an arrangement in space for a collection of atoms, where the inter-atomic force on each atom tends towards zero for a stationary position. It was attained taking into account a tolerance of 2.10^{-5} eV/atom for self-consistency calculations. In addition, other convergence thresholds have been adopted along the successive self stability steps, such as the total energy variation is less than $2{,}10^{-5}$ eV/atom, the maximum force per atom is less than 0,05 eV/Å, the pressure is below 0,1 GPa, and the maximum atomic displacement is less than 2 10^{-3}Å. After acquisition the geometry optimization, the Kohn-Sham electron domain structure was evaluated as well as the partial density of state (PDOS per atom) of the rhombus $C_{14}H_{12}Br_2S_3$ along the high symmetry points of the Brillouin zone. The calculation of optical absorption, dielectric function, optical conductivity, refractive index and loss function for polarized light along the direction [0 0 1] of a crystal is obtained in references [18,19]. Moreover, the electronic and optical properties of the $C_{14}H_{12}Br_2S_3$ crystal have been separately acquired for GGA/PW91 and LDA/CA-PZ, adopting a cutoff energy and k-points of (600 eV, 8 × 8 × 8) and (600eV, 8 × 8 × 8).

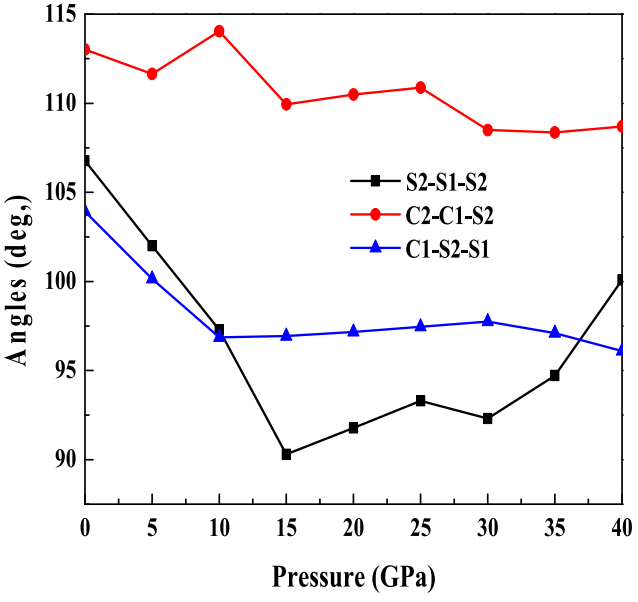

Fig. 4 – The effect of pressure on the most important angles in the phase change between the different atoms in the molecule.

3. Results and discussions

3.1. *Structural properties*

The crystal structure of $C_{14}H_{12}Br_2S_3$ is orthorhombic with space group $P2_12_12$ (No.18), where the conventional unit cell contains 62 atoms. The atomic coordinates of $C_{14}H_{12}Br_2S_3$ computed using LDA/CA-PZ are listed in Table 1 and compared with available experimental ones [1]. The results show an acceptable agreement between the LDA/CA-PZ calculation and available experimental ones. The effect of LDA/CA-PZ, E_{cut} = 240 eV and k-5x5x5, GGA/PBE, E_{cut} = 600 eV and k-8x8x8 and GGA/PW91, E_{cut} = 600 eV and k-8x8x8 on lattice parameters *a*, *b*, *c*, ratios *c*/*a* and *c*/*b*, volume cell, atomic number, density and energy are reported in Table 2. For the lattice parameters, the LDA/CA-PZ gives lower error (0.9%–4.5%) follows by GGA/PBE (1.3%–5.6%) and GGA/PW91 (1.1%–5.9%). All these quantities are closer to the

Table 3 – Atomic populations (Mulliken) of all electrons configurations of atoms for the $2C_{14}H_{12}Br_2S_3$ molecule.

Species	S: Orbitals	P: Orbitals	Total	Charge (e)
H	0.68 to 0.75	0.00	0.68 to 0.75	0.25 to 0.32
C	1.06 to 1.33	2.95 to 3.33	4.01 to 4.66	−0.02 to −0.65
Br	1.64	5.07	6.71	0.29
S	1.84 to 1.87	4.10 to 4.15	5.94 to 6.03	−0.03 to 0.06

Mulliken charges for each atom of $2C_{14}H_{12}Br_2S_3$ in the unit cell were obtained, with the carboxyl group having a charge of (−0.02e to −0.65e), the H group with (0.25e to 0.32e), Br (0.29e) and S (−0.03e to 0.06e).

Table 4 – Geometric parameters of $2C_{14}H_{12}Br_2S_3$, and their experimental values.

Bond	Population	Length (Å)	Exp. (Å) [1]
Br-C	0.41	1.894	1.91
H-C	0.92 to 0.87	1.094 to 1.097	0.95 to 0.99
S-S	0.36	2.036	2.04
C-C	1.17 to 0.82	1.386 to 1.486	1.358 to 1.496
S-C	0.45	1.82	1.82

experimental values. We investigated the effect of $E_{cut\ off}$, k-points and functional type on structural parameters and stability. The GGA/PW91, E_{cut} = 600 eV and k-8x8x8 gives the more stable $C_{14}H_{12}Br_2S_3$ molecule (−7867.948 eV), while, LDA/CA-PZ, E_{cut} = 240 eV and k-5x5x5 report the more accurate lattice parameters. The calculated ratios *c/a* and c/b (0.3945, 0.3875) [0.4014, 0.3762] using (LDA/CA-PZ) [GGA/PW91], agree reasonably with the experimental data (0.393, 0.3656). Fig. 1 shows the unit cell of the orthorhombic crystal $C_{14}H_{12}Br_2S_3$. The zwitterionic molecule $C_{14}H_{12}Br_2S_3$ is visualized in Fig. 2,

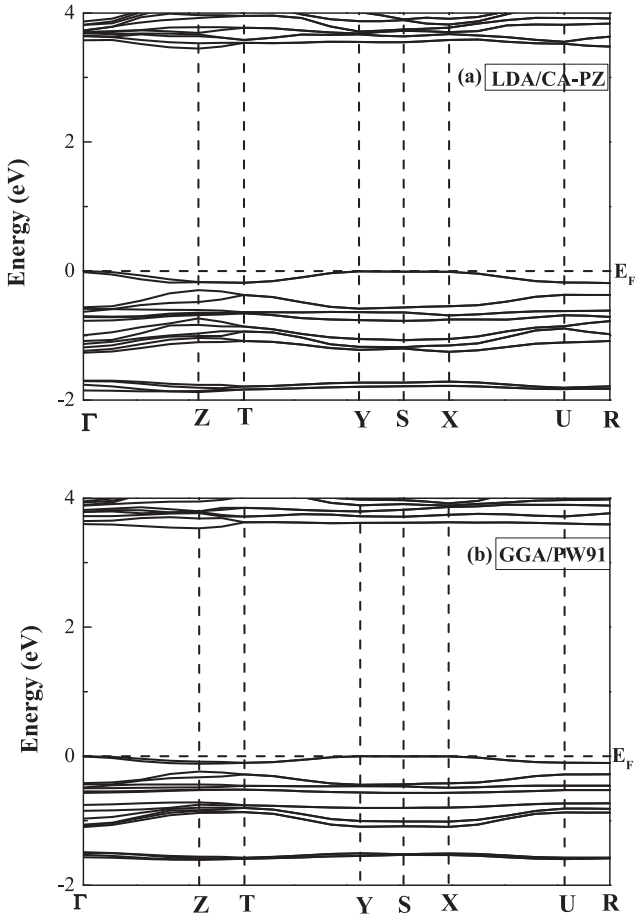

Fig. 5 – Band structures of $C_{14}H_{12}Br_2S_3$ molecule using (a) LDA/AC-PZ and (b) GGA/PW91.

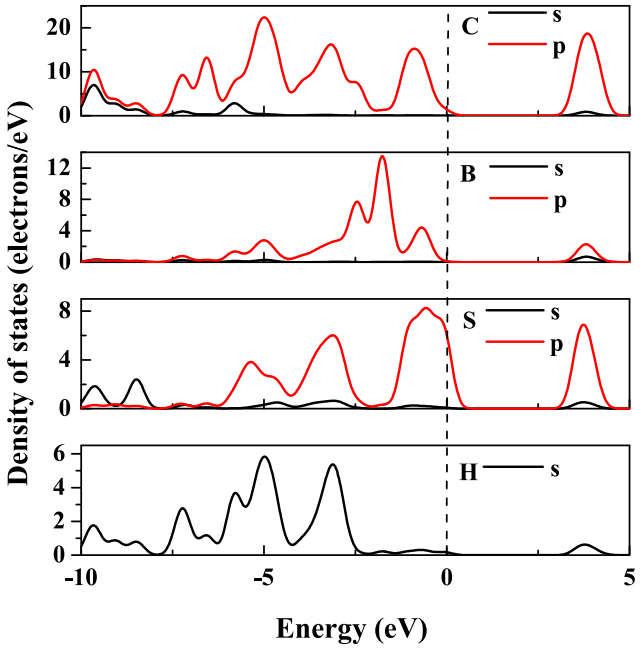

Fig. 6 – The partial density of states of $C_{14}H_{12}Br_2S_3$ molecule.

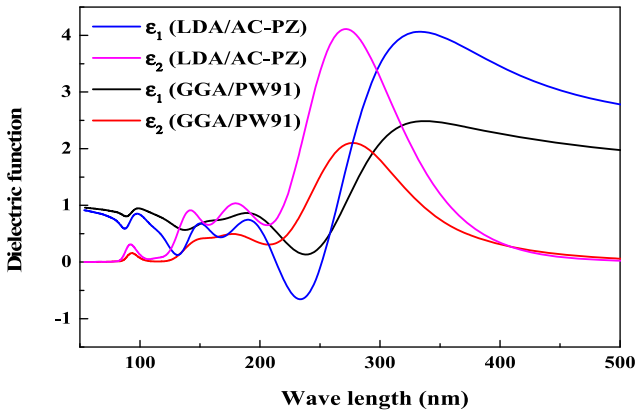

Fig. 7 – The real and imaginary part of the dielectric function of $C_{14}H_{12}Br_2S_3$ molecule.

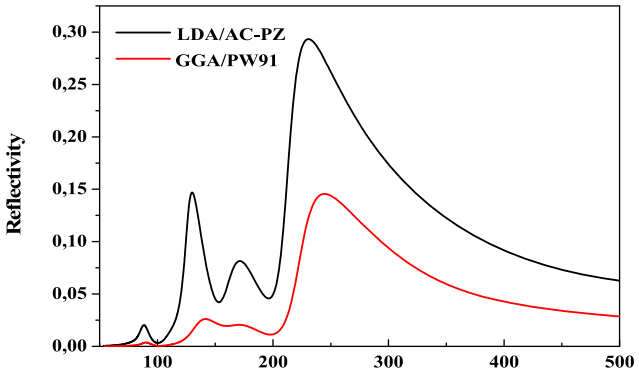

Fig. 8 – The reflectivity of $C_{14}H_{12}Br_2S_3$ as a function of wave length along the direction [1 0 0] with GGA/PW91 and LDA/AC-PZ functional.

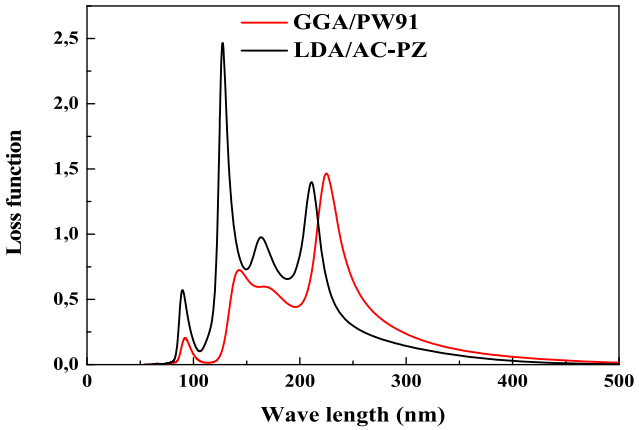

Fig. 10 – The loss function of $C_{14}H_{12}Br_2S_3$ as a function of wave length along the direction [1 0 0] with GGA/PW91 and LDA/AC-PZ functional.

where the shortest distances (Å) are represented. While the perspective view of orthorhombic unit cell in the super-cell is plotted in Fig. 3. The effect of pressure on the most important angles S2-S1-S2, C2-C1-S2 and C1-S2-S1 between the different atoms in the molecule is shown in Fig. 4. This effect is found to be greater in the case of low pressure.

3.2. *Population analysis*

The physical mechanism of interaction between atoms is not lucid. Theoretical calculations based on population analysis [20,21] show that this mechanism is electrostatic in nature. A thorough study of the solid state structure of $2C_{14}H_{12}Br_2S_3$ reveals an intermolecular and intramolecular interaction containing carbon centers. Table 3 summarizes the electronic population of the different atomic sites for the molecule $2C_{14}H_{12}Br_2S_3$. Mulliken charges for each atom of $2C_{14}H_{12}Br_2S_3$ in the unit cell were obtained, with the carboxyl group having a charge of (−0.02e to −0.65e), the H group with (0.25e to 0.32e), Br (0.29e) and S (−0.03e to 0.06e). The results present the aspect of the metal–ligand interaction and the different charge transfers occurring during redox processes to know Mulliken Population Analysis (MPA). Table 4 shows the electronic population in the different atomic bonds and their distances. It is also reported the contesting S-S intramolecular interactions, the weak S-H bonding, the strong S-S intermolecular interactions amongst pairs of diastereo-isomers of $2C_{14}H_{12}Br_2S_3$ and some strong intermolecular interactions between Br atoms and S atoms of the SCH groups, which contribute in the packing of the crystal of $2C_{14}H_{12}Br_2S_3$.

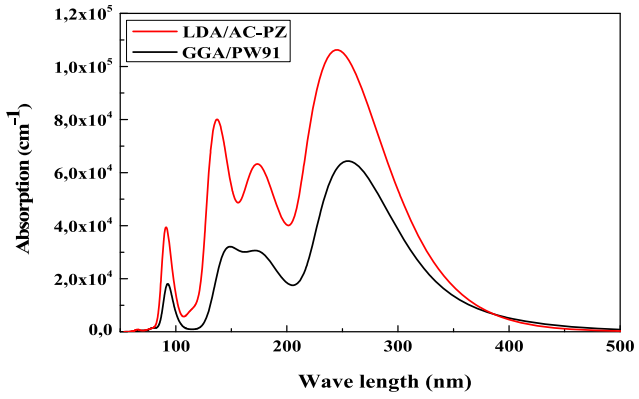

Fig. 9 – The absorption of $C_{14}H_{12}Br_2S_3$ as a function of wave length along the direction [1 0 0] with GGA/PW91 and LDA/AC-PZ functional.

3.3. *Electronic properties*

The electronic band structures are constructed along the lines of high symmetry following the main directions of the Brillouin zone in the reciprocal space. These lines join the following points of high symmetry in terms of unit vectors of the reciprocal space. Γ(0; 0; 0); Z (0; 0; 0.5); T (-0.5; 0; 0.5); Y (-0.5; 0; 0); S (-0.5; 0.5; 0); X (0; 0.5; 0); U (0; 0.5; 0.5); R (-0.5; 0.5; 0.5). Fig. 5 (a, b) represents the computed band structures of $2C_{14}H_{12}Br_2S_3$ crystal with taking into account the scissor operator. It is noted a large indirect band gap Z→Γ (3.4498 eV and 3.5319 eV) using LDA/AC-PZ and GGA/PW91 approaches, since the maximum of the valence band and the minimum of the conduction band are offset from each other in the Brillouin zone. The top of the valence band is chosen at 0 eV and

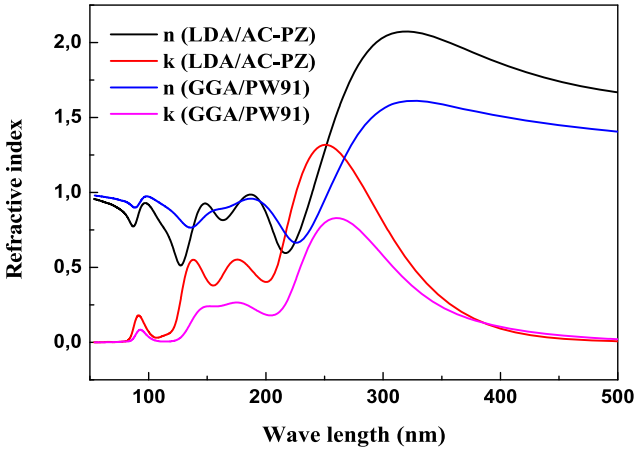

Fig. 11 – The refractive index of $C_{14}H_{12}Br_2S_3$ as a function of wave length along the direction [1 0 0] with GGA/PW91 and LDA/AC-PZ functional.

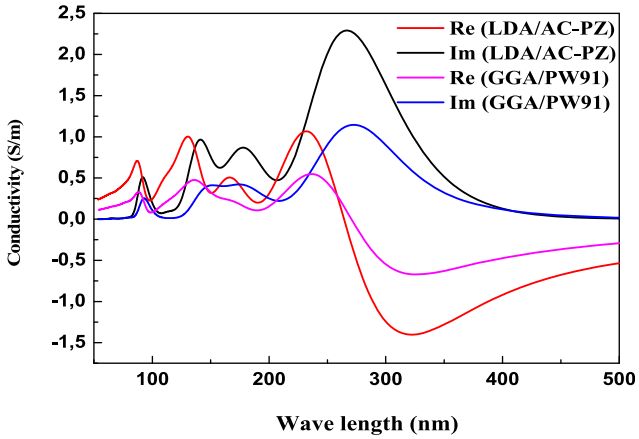

Fig. 12 – The conductivity of $C_{14}H_{12}Br_2S_3$ as a function of wave length along the direction [1 0 0] with GGA/PW91 and LDA/AC-PZ functional.

designated the Fermi level E_F. The levels of the valence band are continuous especially along the line Γ-Z-T to the Brillouin zone. This continuum forms a set of narrow sub-bands, particularly along the U-R line to the Brillouin zone. $C_{14}H_{12}Br_2S_3$ molecule is characterized by a wide band gap, which separates the last occupied states of the valence band and the free states of the conduction band. In the range 0 and -2 eV, the valence band consists of four zones separated by a gap. The upper valence band is located at −0.1821 eV and −0.1166 eV for LDA/AC-PZ and GGA/PW91. From the qualitative agreement of the LDA/AC-PZ and GGA/PW91 approaches for band structures with some variances in the band gap of the crystal $C_{14}H_{12}Br_2S_3$, we predicted two indirect band gap of energies 3.46 eV, 3.51 eV (3.54 eV, 3.97 eV) for GGA/PW91 (LDA/AC-PZ). The partial densities of the electronic states that give the individual contribution of atoms are calculated for the diagram of the energy bands E (k) of the crystalline structure of $C_{14}H_{12}Br_2S_3$ as shown in Fig. 6. The electronic contribution in the upper valence band comes from S: p, C: p and B: p states. The first conduction band is empty and the transitions occur from S: p, C: p and B: to all others sites, There are hybridizations in the upper valence band between S: p, B: p and C: p, therefore, there is a covalent bonding corresponding to the cited states. Other hybridization between H: s, S: p and C: p is located in the range −2.3 eV to −4.12 eV. The narrow peaks in the conduction band are subjugated by C: p, B: p and S: p states with a small contribution of H: s site.

3.4. *Optical properties*

The study of the optical properties of materials is important to observe their response when they interact with energy and allow the understanding of electronic structure. A polarized incident light in the direction [100] on an orthorhombic crystal $C_{14}H_{12}Br_2S_3$ is considered as an energy source. We begin by the complex dielectric function which is the sum of a real part and another imaginary $\varepsilon(\omega) = \varepsilon_1(\omega) + \varepsilon_1(\omega)$. The real part translates the optical response and the imaginary part show the reflectivity of the material. The real and imaginary parts of the dielectric function of $C_{14}H_{12}Br_2S_3$ molecule are drawn in Fig. 7.

The static dielectric constant of $C_{14}H_{12}Br_2S_3$ is 0.91 and 0.95 for LDA/CA-PZ and GGA/PW91. The maximum value is observed at a wave length of 333 nm, which show the higher optical response in the ultraviolet domain. It is observed that for photons wave length 235.5 nm, the real part of dielectric function becomes negative; but always larger than −1, hence, peak is obtained for LDA/CA-PZ and also showing metallic nature. For a metal, if the frequency is lower, the real part is negative meaning that the light is completely reflected. The electrons around the surface can screen the electric fields of the light before it gets into the bulk. But if the frequency is higher than the plasmon frequency, the real part is positive and the metal behaves like a dielectric medium.

The reflectivity of any material is calculated by dielectric function through the equation:

$$R(\omega) = \left|\frac{(\varepsilon_1)^{1/2} - 1}{(\varepsilon_1)^{1/2} + 1}\right| \quad (1)$$

The reflectivity is inversely proportional to the absorption coefficients and it depends on the incident photon energy. When more light is absorbed in any material then reflection is less. The reflectivity as function of wave length is shown in Fig. 8. The maximum of reflectivity of 0.29 and 0.14 at 231.4 nm and 244.6 nm is observed for LDA/AC-PZ and GGA/PW91. The reflectivity is more important in the LDA/AC-PZ case. The reflectivity is observed only in the ultraviolet light domain. Fig. 9 portrays the spectrum of optical absorption of $C_{14}H_{12}Br_2S_3$ molecule along the polarization direction [001] for the GGA/PW91 and LDA/AC-PZ approaches. The results obtained on absorption show that the $C_{14}H_{12}Br_2S_3$ crystal absorbs photonic energy in the ultraviolet range (70 nm–400 nm), which corresponds to the energy range 3.11 eV–17.75 eV. The absorption is more important in the LDA/AC-PZ approach. The maximum of absorption is 106220 cm^{-1} (64364 cm^{-1}) at 246.4 nm (256.5 nm) for LDA/AC-PZ (GGA/PW91). The absorption through the electrons and photons interactions results because inter band and intra band transitions. The absorption increases and reaches two maxima at 130 nm and 233 nm (243 nm) for LDA/AC-PZ (GGA/PW91) in the wavelength range (60 nm–500 nm); this means that the $C_{14}H_{12}Br_2S_3$ crystal is a potential candidate as coating material in this range. The loss function describes the interaction of a very fast moving electron travelling with loss of energy throughout the material. These interactions may be phonon excitation, intraband and interband transitions, Plasmon excitations and inner shell ionization. The loss function is calculated through the equation:

$$L(\omega) = \frac{\varepsilon_2(\omega)}{\varepsilon_1^2(\omega) + \varepsilon_2^2(\omega)} \quad (2)$$

The loss of energy is low at small and high wave length values but the maximum loss of energy is at 127.45 nm as we shown in Fig. 10. There are several plasmon peaks in the crystal structure. The extinction coefficient and refractive index can be obtained through the complex dielectric constant. The absorption and refraction of a medium are described with single quantity called the complex refractive index. The equations of refractive index (real part) and extinction coefficient (imaginary part) are given as:

$$n(\omega)=\frac{\sqrt{2}}{2}\left[\varepsilon_1+\sqrt{\varepsilon_1^2+\varepsilon_2^2}\right] \quad (3)$$

$$k(\omega)=\frac{\sqrt{2}}{2}\left[-\varepsilon_1+\sqrt{\varepsilon_1^2+\varepsilon_2^2}\right]$$

We present the refractive index and extinction coefficient in Fig. 11. We observed that the high peaks for both the extinction coefficient and refractive index beyond 250 eV show the absence of optical response of the material in this region. The peaks of the extinction coefficient and the refractive index are located between the lower and upper bands of the inter-band transition. The optical conductivity $o(\omega)$ is calculated through the imaginary part of dielectric function as:

$$\sigma(\omega)=\frac{\omega}{4\pi}\varepsilon_2(\omega) \quad (4)$$

The conductivity of $C_{14}H_{12}Br_2S_3$ molecule as a function of wave length along the direction [1 0 0] with GGA/PW91 and LDA/AC-PZ functional is reported in Fig. 12. There are a series of peaks of conductivity (real and imaginary part) between 80 nm and 260 nm. The optical conductivity peaks 1.067 S/m and 2.291 S/m (0.547 S/m and 1.146 S/m) are quite high at wave length 266.7 nm and 229.5 nm (236.1 nm and 272.4 nm) for LDA/AC-PZ (GGA/PW91). The real part of conductivity becomes negative beyond 271.3 nm (264.7 nm) for GGA/PW91 (LDA/AC-PZ). The real part of the conductivity becomes negative beyond the resonance frequency. This is a typical resonance behavior and implies that when the imaginary part vanishes the response is 180° out of phase with the applied magnetic field.

4. Conclusion

An ab-initio study on geometry optimization, electronic band structure and density of states, dielectric function, optical absorption and conductivity have presented for $2C_{14}H_{12}Br_2S_3$ anhydrous crystals. The equilibrium lattice parameters of $2C_{14}H_{12}Br_2S_3$ obtained in this work are closer to available theoretical and experimental values quoted in the literature. Mulliken charges for each atom of $2C_{14}H_{12}Br_2S_3$ in the unit cell were obtained, with the carboxyl group having a charge of (−0.02e to −0.65e), the H group with (0.25e to 0.32e), Br (0.29e) and S (−0.03e to 0.06e). The real part of dielectric function value for LDA/CA-PZ at wave length between 213.5 nm and 252.2 nm becomes negative and translates the metallic nature of $2C_{14}H_{12}Br_2S_3$. The $C_{14}H_{12}Br_2S_3$ crystal absorbs photonic energy in the ultraviolet range (70–400 nm), which corresponds to the energy range 3.11–17.75 eV, and such crystal is a potential candidate as coating material in this range. We investigated the effect of $E_{cut\ off}$, k-points and LDA/CA-PZ, GGA/PBE and GGA/PW91 functional on lattice parameters and stability. The physical mechanism of interaction between atoms in $2C_{14}H_{12}Br_2S_3$ molecule is electrostatic type in nature. The study of $2C_{14}H_{12}Br_2S_3$ at solid state structure reveals the intermolecular and intramolecular interactions containing carbon centers. Mulliken population analysis shows S-S intramolecular interactions, weaker S-H bonding, stronger S-S intermolecular interaction and Br-S intermolecular interaction amongst pairs of diastereo-isomers of $2C_{14}H_{12}Br_2S_3$. The pressure effect on the angles S2-S1-S2, C2-C1-S2 and C1-S2-S1 between the different atoms in the molecule is investigated. The hybridizations in the upper valence band between S: p, B: p and C: p, translates their covalent bonding.

Declaration of Competing Interest

The authors declare that they have no known competing financial interests or personal relationships that could have appeared to influence the work reported in this paper.

Acknowledgments

We would like to thank Taif University Research Supporting Project number (TURSP-2020/66), Taif University, Taif, Saudi Arabia.

REFERENCES

[1] Singh Sunnel P, Lough Alan J, Shwan Adrian L. Crystallographic Comunications 2009;65(part 2):361. https://doi.org/10.1107/S1600536809001834.
[2] Bhabak Krishna P, Bhowmick Debasish. J Mol Struct 2012;1022(29):16–24.
[3] Banerji A, Kalena GP. Tetrahedron Lett 1980;21:3003–4.
[4] Nonius COLLECT. Delft, The Netherlands: Nonius BV; 2002.
[5] Abu-Yousef IA, Rys AZ, Harpp DN. J Sulfur Chem 2006;27:15–24.
[6] De Sousa JR, Demuner AJ, Pinheiro JA, Breitmaier E, Cassels BK. Phytochemistry 1990;29:3653–5.
[7] Johnson L, Williams LAD, Roberst EV. Pestic Sci 1997;50:228–32.
[8] Haoyun A, Jenny Z, Xiaobo W, Xiao X. Bioorg Med Chem Lett 2006;16:4826–9.
[9] Clark SJ, Segall MD, Pickard CJ, Hasnip PJ, Probert MJ, Refson K, et al. Zeitschrift fur Kristallographie 2005;220:567–70.
[10] Ceperley DM, Alder BJ. Phys Rev Lett 1980;45:566.
[11] Perdew JP, Zunger A. Phys Rev B 1981;23:5048–79.
[12] Perdew JP, Burke K, Ernzerhof M. Phys Rev Lett 1996;77:3865.
[13] Lin JS, Qteish A, Payne MC, Heine V. Phys Rev B 1993;47:4174.
[14] Monkhorst HJ, Pack JD. Phys Rev B 1976;13:5188–92.
[15] Hohenberg P, Kohn W. Phys Rev 1964;136:B864.
[16] Kohn W, Sham LJ. Phys Rev 1965;140:A1133.
[17] Albuquerque EL, Fulco UL, Freire VN, Caetano EWS, Lyra ML, Moura FABF. Phys Rep 2014;535:139–209.
[18] Zhong M, Liu QJ, Jiang CL, Liu FS, Tang B, Peng XJ. J Phys Chem Solid 2018;121:139–44.
[19] Jubair M, Karim AMMT, Nuruzzaman M, Zilani MAK. J Phys Commun 2019;3:055017.
[20] Bleiholder C, Gleiter R, Werz DB, Koeppel H. Inorg Chem 2007;46:2249–60.
[21] Bleiholder C, Werz DB, Koeppel H, Gleiter RJ. Am Chem Soc 2006;128:2666–74.